Arabian Journal of Chemistry (2011) **4**, 45–49

King Saud University

Arabian Journal of Chemistry

www.ksu.edu.sa
www.sciencedirect.com

ORIGINAL ARTICLE

Electrical conductivity of AgI–CdI_2–KI and AgI–CuI–KI ionic conducting systems

Mohammed Hassan [a,*], **Ahmed Noman Al-hakimi** [a], **Rafiuddin** [b]

[a] *Chemistry Department, Faculty of Science, Ibb University, Ibb, Yemen*
[b] *Physical Chemistry Division, Chemistry Department, Aligarh Muslim University, Aligarh 202 002, India*

Received 10 October 2009; accepted 8 December 2009
Available online 16 June 2010

KEYWORDS
Ionic conductivity;
Impedance spectroscopy;
DSC;
X-ray diffraction

Abstract Samples of general formulae $(AgI)_{4-2x}(CdI_2)_xKI$ and $(AgI)_{4-x}(CuI)_xKI$, x = 0–0.4, have been prepared and studied by conductivity measurements, powder X-ray diffraction and DSC techniques. Room temperature XRD reveals the presence of the orthorhombic K_2AgI_3 as the major component in the system. DSC traces show endothermic peaks in the temperature range of 309–330 K, depending on the sample composition. These are attributed to the solid state reaction between AgI and K_2AgI_3 to form the cubic KAg_4I_5. Impedance spectra show the prominence of electrode – electrolyte interface effect which is explained in terms of the high rate of ion migration. Ionic conductivity enhances with the increase of Cd^{2+} content, while Cu^+ contained samples show a decrease in conductivity with increasing Cu^+ ratio though the ionic conductivity remains higher than that of the pure one.

1. Introduction

Superionic conductors are a class of materials that exhibit exceptionally high ionic conductivity in the solid state. Their wide applications in microbatteries, sensors, smart devices etc. encourage many investigators to study their properties in order to produce improved materials. It was reported that high ionic conductivity in this class occurs by motion of the charge carriers through liquid like lattice (disordered materials) or through channels in layer materials (West, 2003).

AgI is the most investigated superionic conductor which has high ionic conductivity in its α-phase stable above 420 K. Its ionic conductivity was attributed to the highly disordered structure of the phase. Extensive efforts have been made to bring the liquid like structure of this phase to lower temperatures (Knauth and Tuller, 2002; Hull, 2004; Kumar and Yashonath, 2006). Among the strategies which were followed for this purpose, modification of the crystal structure have been done by introducing iso and aliovalent cations in the lattice of the compound (Hull et al., 2002a,b; Brightwell et al., 1984; Hull and Berastegui, 2004).

AgI–KI is one such system in which K^+ ions were incorporated into the lattice of AgI. The phase diagram of the system

---

[*] Corresponding author.
E-mail address: abuusef2002@gmail.com (M. Hassan).

1878-5352 © 2010 King Saud University. All rights reserved. Peer-review under responsibility of King Saud University.
doi:10.1016/j.arabjc.2010.06.017

Production and hosting by Elsevier

was studied by many authors (Bradley and Green, 1966a,b; Topol and Owens, 1968). All studies indicated the presence of a highly conducting compound of the formula KAg_4I_5 and a non conducting one of the formula K_2AgI_3. The structures of the two compounds are to be primitive cubic and orthorhombic unit cells respectively (Brink and Kores, 1952; Bradley and Green, 1967).

In this paper, the ionic conductivity of the two systems $(AgI)_{4-2x}(CdI_2)_xKI$ and $(AgI)_{4-x}(CuI)_xKI$, $x = 0–0.4$, is being investigated. Cu^+ ion may enhance the ionic conductivity by its participation in the conduction process. Ionic conductivity can also be promoted by introducing divalent Cd^{2+} ion which results in increasing vacancy concentration in the lattice and hence facilitating the motion of the mobile cation Ag^+. Moreover, Ag_4KI_5 was reported to be stable above ≈309 K and below this temperature disproportionates to AgI and AgK_2I_3 (Bradley and Green, 1966a). The introduction of different ions into the system with keeping the stochiometry of the compound may modify the structure and stabilizes it at ambient temperature.

2. Experimental

2.1. Materials and instrumentation

AgI was prepared by precipitation using AR grade $AgNO_3$ and KI. CuI and CdI_2 were taken from Ottockemi and Loba-Cheme, India, respectively, with the stated purity of 99%. The required amounts of the raw materials were mixed in an agate mortar for an hour to prepare the two series $(AgI)_{4-2x}(CdI_2)_x$-KI and $(AgI)_{4-x}(CuI)_xKI$, $x = 0–0.4$, followed by heating at 473 K for 48 h. The slowly cooled materials were then crushed to fine powder. The powder materials were white coloured at the time of preparation and turned to yellow when left in the atmosphere, hence they were kept in perfectly closed glass tubes till the time of analysis.

Themogravimetric analysis of the samples showed weight loss due to moisture content of less than 1.5% at about 473 K. Circular pellets of 4.524 cm^2 surface area and 0.1 cm thickness were made by hydraulic press machine at a pressure of about 4 tonnes/cm^2. The conductivity and capacitance measurements were performed by means of the two probe method. The pellet was mounted on stainless steel holder between copper leads using two polished platinum electrodes. The copper leads were insulated from the sample holder by Teflon sheets. The pellet was annealed at 310 K between the platinum electrodes for 8 h to increase the electrical contact and to minimize the grain boundary effects.

The electrical measurements were done in the temperature range of 303–473 K using GenRad 1659 RLC Digbridge at a fixed frequency of 1 kHz. The heating rate was maintained at 0.5 K/min. Our measurements at this frequency were found to be in the same order as those reported previously using different technique, though the electrodes were different in the two studies (Roy et al., 1982). DSC scanning was traced by Perkin Elmer instrument using Alumina powder as a reference and measured the temperature with the accuracy of ±0.5 K. The heating rate was kept at 10 K/min. Impedance measurements were performed using HIOKI3532-50 LCR meter in the frequency range of 40 Hz–5 MHz. Room temperature XRD was done by RIGAKU D/MAX-B diffractometer with CuK_α radiation.

3. Results and discussion

3.1. X-ray and DSC

X-ray diffractograms of the samples taken at room temperature are presented in Figs. 1 and 2. These figures show the presence of a prominent phase which is orthorhombic AgK_2I_3 in Cu^+ substituted samples while AgI was the prominent. Phase in the case of Cd^{2+} substituted ones. The lattice constants of the orthorhombic phase were calculated using Powder x program and presented in Table 1.

There is a good agreement between these values and those reported previously (Hull and Berastegui, 2004; Bradley and Green, 1966a; Brink and Kores, 1952). No peaks related to Ag_4KI_5 were detected. Peaks with a very low intensity were observed and hence can be attributed to the substituents, CuI and CdI_2, which were not incorporated into the lattice of AgK_2I_3. These results are consistent with those of the previous investigations which indicate that disproportion of Ag_4KI_5 occurs below 309 K to AgI and AgK_2I_3.

DSC traces of the samples are depicted in Fig. 3. DSC curve of the pure material ($x = 0$) show two arrests, the first is a little broad initiated at 309 K and the second is sharp at 527 K. The former is for the occurrence of the reaction between AgI and AgK_2I_3 to form Ag_4KI_5, and the latter is for the incongruent melting of Ag_4KI_5. The DSC curves for the substituted samples show the first thermal arrest in the temperature range of 313–328 K and the second in the range of 517–529 K.

Thermal arrests are also observed in DSC curves of most of the Cd^{2+} and Cu^+ contained samples in the temperature range of 415–439 K and these are related to small amounts of AgI. Hence, Ag_4KI_5 got destabilized upon incorporation of foreign ions into its lattice. The substitution has stabilized AgK_2I_3 other than the target compound. This may be due to the Cu^+ and Cd^{2+} being smaller in size than Ag^+ and can be accommodated easily by the smaller size lattice of AgK_2I_3. The temperatures corresponding to these arrests are summarized in Table 2.

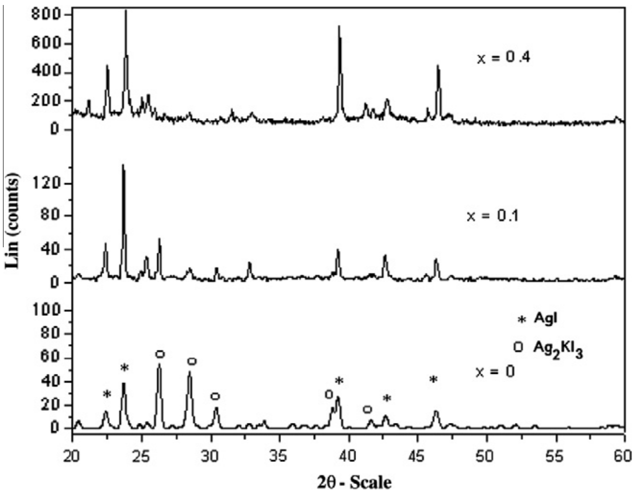

Figure 1 Room temperature XRD diffractograms of $(AgI)_{4-2x}(CdI_2)_xKI$ samples.

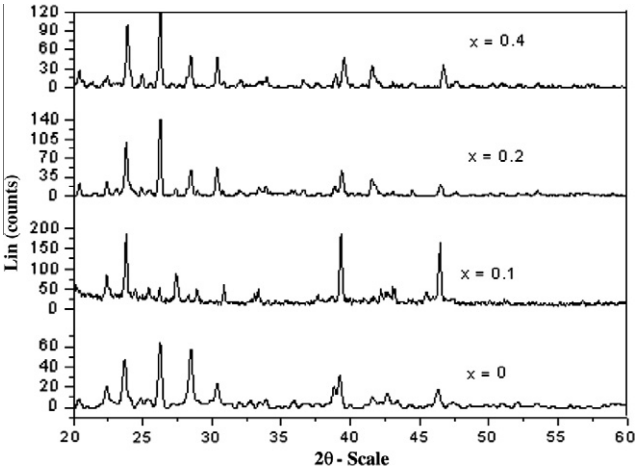

Figure 2 Room temperature XRD diffractograms of $(AgI)_{4-x}(CuI)_xKI$ samples.

Table 1 Calculated lattice parameters of the orthorhombic phase Ag_2KI_3 formed at room temperature in the $(AgI)_{4-2x}(CdI_2)_xKI$ and $(AgI)_{4-x}(CuI)_xKI$ samples.

Sample	a (Å)	b (Å)	c (Å)
$x = 0$	9.921	4.720	19.473
$(AgI)_{3.8}(CdI_2)_{0.1}KI$	10.000	4.760	19.468
$(AgI)_{3.6}(CdI_2)_{0.2}KI$	9.995	4.832	19.456
$(AgI)_{3.9}(CuI)_{0.1}KI$	9.778	4.731	19.507
$(AgI)_{3.8}(CuI)_{0.2}KI$	9.879	4.746	19.469
$(AgI)_{3.6}(CuI)_{0.4}KI$	9.999	4.746	19.300

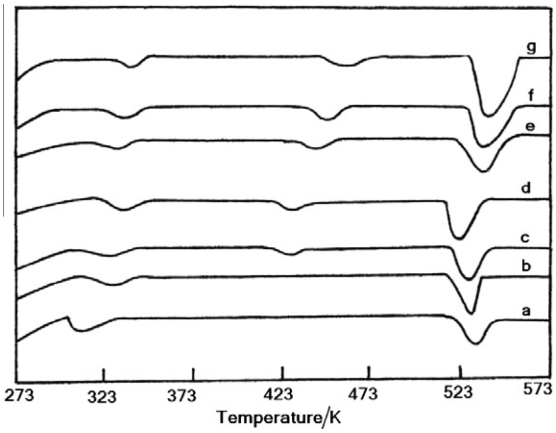

Figure 3 DSC curves of $(AgI)_{4-2x}(CdI_2)_xKI$ and $(AgI)_{4-x}(CuI)_xKI$ samples: (a) $x = 0$, (b) $(AgI)_{3.8}(CdI_2)_{0.1}KI$, (c) $(AgI)_{3.6}(CdI_2)_{0.2}KI$, (d) $(AgI)_{3.2}(CdI_2)_{0.4}KI$, (e) $(AgI)_{3.9}(CuI)_{0.1}KI$, (f) $(AgI)_{3.8}(CuI)_{0.1}$ KI, g. $(AgI)_{3.6}(CuI)_{0.4}KI$.

Bradley et al. Bradley and Green (1966a) observed broad peak in his DSC and indicated the occurrence of the following two reactions:

$$7AgI + AgK_2I_3 \leftrightarrow 2Ag_4KI_5 \tag{1}$$

$$4AgK_2I_3 \leftrightarrow Ag_4KI_5 + 7KI \tag{2}$$

However our measurements show only one peak with intermediate broadness initiated at 309 K. No other peaks are observed in the temperature range 403–413 K as indicated by Bradley et al. It is therefore suggested that the occurrence of only one reaction, the first one since AgI was detected in the X-ray powder analysis.

3.2. Electrical conductivity

In the complex impedance plot for the pure sample, $x = 0$, Fig. 4 shows a spike at lower frequency and small part of a depressed semicircle at higher frequencies. The spike is related to the interfacial effects between the electrode and electrolyte while the semicircle can be attributed to the bulk resistance of the samples assuming the grain boundary effect to be the minor. The Cd^{2+} and Cu^{+} contained samples show similar behavior with the difference that the spike is now extended to the higher range of frequencies and no part of the semicircle is seen within the limits of our measurements.

These results indicated very high diffusive trend of the mobile ions resulting in space-charge layer causing this type of impedance behavior known as Warburg impedance. This behavior is normal for high conducting phases and has been observed in many materials (Ahmed, 2006).

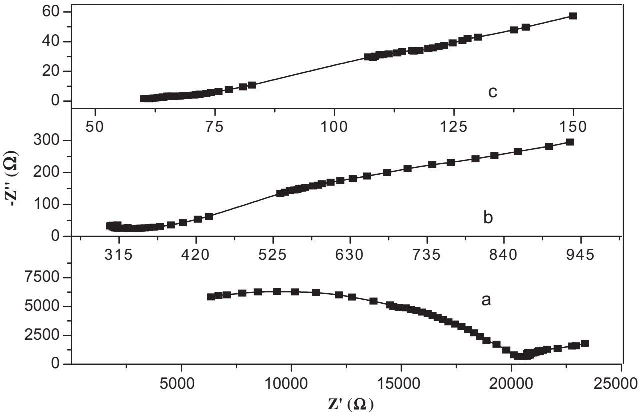

Figure 4 Complex impedance plots of $(AgI)_{4-2x}(CdI_2)_xKI$ and $(AgI)_{4-x}(CuI)_xKI$ samples: (a) $x = 0$, (b) $(AgI)_{3.4}(CdI_2)_{0.3}KI$ and (c) $(AgI)_{3.7}(CuI)_{0.3}KI$.

Table 2 Transition temperatures to the cubic Ag_4KI_5 phase and congruent melting points of the $(AgI)_{4-2x}(CdI_2)_xKI$ and $(AgI)_{4-x}(CuI)_xKI$ samples.

Sample	Transition temperature (K)	Melting point (K)	Sample	Transition temperature (K)	Melting point (K)
$x = 0$	309	527	$(AgI)_{3.9}(CuI)_{0.1}KI$	316	528
$(AgI)_{3.8}(CdI_2)_{0.1}KI$	318	525	$(AgI)_{3.8}(CuI)_{0.2}KI$	316	528
$(AgI)_{3.6}(CdI_2)_{0.2}KI$	325	523	$(AgI)_{3.6}(CuI)_{0.4}KI$	316	528
$(AgI)_{3.2}(CdI_2)_{0.4}KI$	333	516			

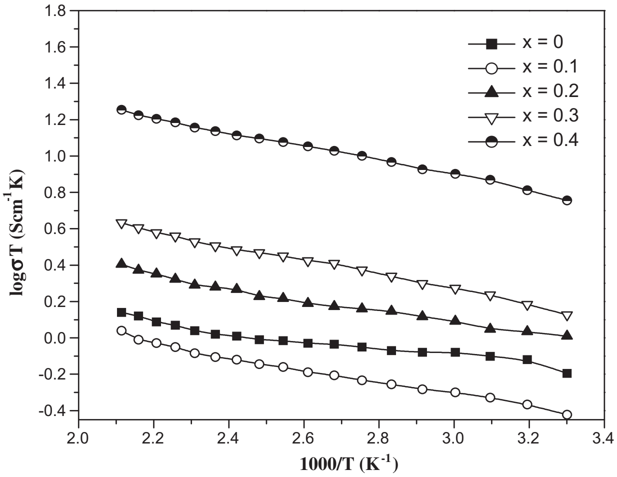

Figure 5 Ionic conductivity at 1 kHz of $(AgI)_{4-2x}(CdI_2)_xKI$ samples as a function of temperature.

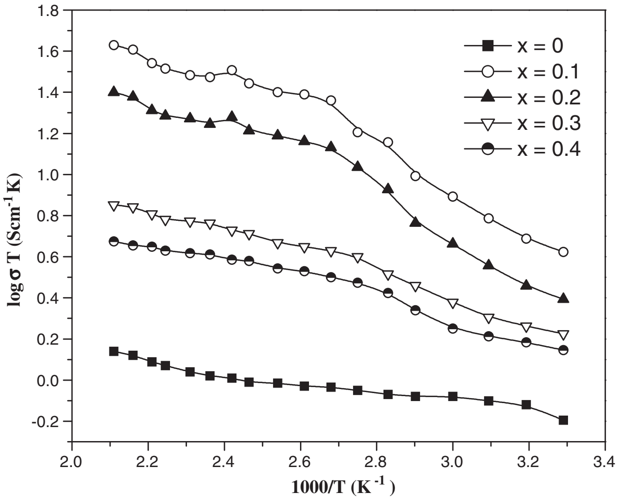

Figure 6 Ionic conductivity at 1 kHz of $(AgI)_{4-x}(CuI)_xKI$ samples as a function of temperature.

The temperature dependence of ionic conductivity for pure, Cd^+ and Cu^+ contained samples (Figs. 5 and 6) is given by the Arrhenius expression,

$$\sigma = \sigma_0 \exp(-E_a/kT) \tag{3}$$

where σ_0 is the pre-exponential factor and E_a is the activation energy of ionic motion. Addition of low concentration of Cd^{+2} ($x = 0.1$) into the system has decreased the ionic conductivity (Fig. 5), while the incorporation of higher concentration of Cd^+ ($x = 0.2$–0.4) leads to the enhancement of the ionic conductivities beyond that of the pure compound. The conductivity increases gradually with increasing Cd^{2+} content. This is expected because the introduction of non-mobile divalent cation Cd^{2+} has two opposite effects; the first is diminishing the ionic conductivity due to the decrease in the number of charge carriers Ag^+ ions in the lattice, secondly, promotion of the ionic conductivity by increasing the vacancy concentration due to the charge compensation. The first effect is prominent at lower concentration of Cd^{2+} while the second effect is important when the concentration is $x \geqslant 0.2$. This behavior is well observed in related works (Ravi et al., 1993; Padmasree et al., 2005; Nair et al., 1996).

Ionic conductivity in Cu^+ contained samples (Fig. 6) got enhanced; however, it has decreased with further increase of the Cu^+ content. The enhancement of ionic conductivity resulted either from an increased concentration of the crystalline defects or from the increased free volume which results from copper ions entering the lattice (Beeken et al., 2002). Small rise in the conductivity was observed in the temperature.

Range 333–353 K which is also seen as a broad endothermic arrest at about this range. Sevanesan and Gobinathan (Sevanisan and Gobinathan, 1990) have observed this change as a knee in the conductivity curves of all compositions in the system AgI–CuI–KI in the temperature range 328–350 K. This peak corresponds to phase change occurs within the sample. This might have been initiated at lower temperature than 333 K but, due to the slow rate of the reaction, it was observed only at higher temperature in the conductivity measurements. Activation energies calculated from the slope of Arrhenius plots are presented in Table 3. The activation energy of conduction in the sample where $x = 0$ is found to be in excellent agreement with the value reported previously (Roy et al., 1982) while Cd^{2+} and Cu^+ contained samples show higher activation energies. The smaller sizes of Cu^+ and Cd^{+2} cause contraction of the lattice which lead to the decrease of the bottle neck size through which hopping of the mobile ions takes place resulting in higher activation energies in the Cd^{2+} and Cu^+ contained samples. However, the activation energy decreases gradually on increasing ion concentration in the system. This is due to the higher concentration of defects which facilitates the ionic diffusion at higher concentration of the added ions. This behavior is in agreement with those observed in similar investigations (Beeken and Beeken, 2000; Beeken et al., 1994).

4. Conclusion

The effect of addition of CdI_2 and CuI to the system AgI–KI was investigated in an attempt to enhance the ionic conduction and stabilize the compound Ag_4KI_5 at ambient temperature. The first target was achieved by getting higher ionic conductivity in CdI_2 and CuI contained samples, while the second could

Table 3 Activation energies of conduction of the $(AgI)_{4-2x}(CdI_2)_xKI$ and $(AgI)_{4-x}(CuI)_xKI$ samples.

Sample	Activation energy of conduction (eV)	Sample	Activation energy of conduction (eV)
A_4KI_5	0.045	$(AgI)_{3.9}(CuI)_{0.1}KI$	0.171
$(AgI)_{3.8}(CdI_2)_{0.1}KI$	0.069	$(AgI)_{3.8}(CuI)_{0.2}KI$	0.170
$(AgI)_{3.6}(CdI_2)_{0.2}KI$	0.065	$(AgI)_{3.7}(CuI)_{0.3}KI$	0.108
$(AgI)_{3.4}(CdI_2)_{0.3}KI$	0.064	$(AgI)_{3.6}(CuI)_{0.4}KI$	0.093
$(AgI)_{3.2}(CdI_2)_{0.4}KI$	0.062		

not be obtained. Impedance spectra show the prominence of electrode–electrolyte interface effect due to the high level of structural disorders.

References

Ahmed, M.M., 2006. Solid State Ionics 177, 21.

Beeken, R.B., Beeken, E.M., 2000. Solid State Ionics 136–137, 463.

Beeken, R.B., Jetzer, W.L., Smith, D.R., 1994. Solid State Ionics 70–71, 176.

Beeken, R.B., Faludi, J.C., Schreir, W.M., Tritz, J.M., 2002. Solid State Ionics 154–155, 719.

Bradley, J.N., Green, P.D., 1966a. Trans. Faraday Soc. 62, 2069.

Bradley, J.N., Green, P.D., 1966b. Trans. Faraday Soc. 63, 424.

Bradley, J.N., Green, P.D., 1967. Trans. Faraday Soc. 63, 2516.

Brightwell, J.W., Buckley, C.N., Hollyoak, R.C., Ray, B., 1984. J. Mater. Sci. Lett. 3, 443.

Brink, C., Kores, H.A.S., 1952. Acta. cryst. 15, 433.

Hull, S., 2004. Rep. Prog. Phys. 67, 1233.

Hull, S., Berastegui, P., 2004. J. Solid State Chem. 177, 3156.

Hull, S., Keen, D.A., Sivia, D.S., Berastegui, P., 2002a. J. Solid State Chem. 165, 363.

Hull, S., Keen, D.A., Berastegui, P., 2002b. J. Phys.: Condens. Matter 14, 13579.

Knauth, P., Tuller, H.L., 2002. J. Am. Ceram. Soc. 85, 1654.

Kumar, P.P., Yashonath, S., 2006. J. Chem. Sci. 118, 135.

Nair, S.M., Yehia, A.I., Ahmad, A., 1996. J. Solid State Chem. 122, 349.

Padmasree, K.P., Kanchan, D.K., Panchal, H.R., Awasth, A.M., Bharadwaj, S., 2005. Solid State Commun. 136, 102.

Ravi, B.G., Ramasamy, S., Baskaram, N., 1993. J. Mater. Sci. Lett. 12, 464.

Roy, S.K., Sridaran, P., Bhuniya, R.C., 1982. J. Mater. Sci. Lett. 1, 536.

Sevanisan, S., Gobinathan, R., 1990. J. Mater. Sci. Lett. 9, 62.

Topol, L.E., Owens, B.B., 1968. J. Phys. Chem. 72, 2106.

West, A.R., 2003. Solid State Chemistry and Its Applications. Wily, Singapore, pp. 453.